

AD-A051 853

DEFENCE RESEARCH ESTABLISHMENT VALCARTIER (QUEBEC)

F/G 20/5

FREQUENCY AND AMPLITUDE CHARACTERISTICS OF A HIGH-REPETITION-RA--ETC(U)

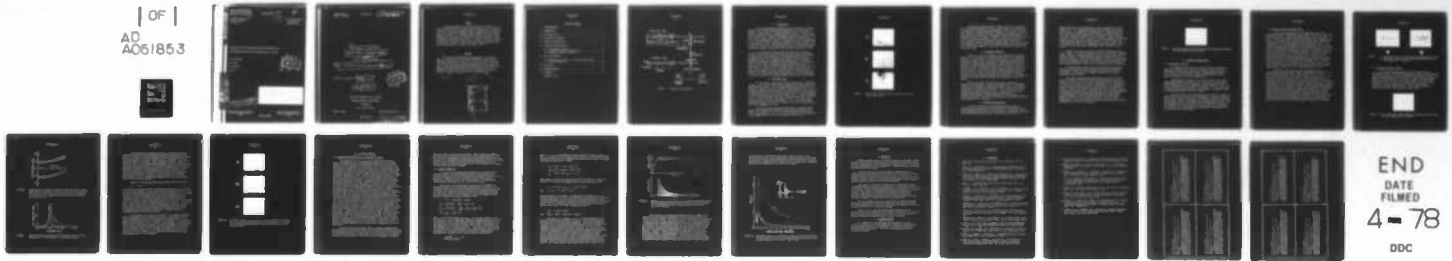
FEB 78 J - LACHAMBRE, P LAVIGNE, M VERREAULT

UNCLASSIFIED

DREV-R-4091/78

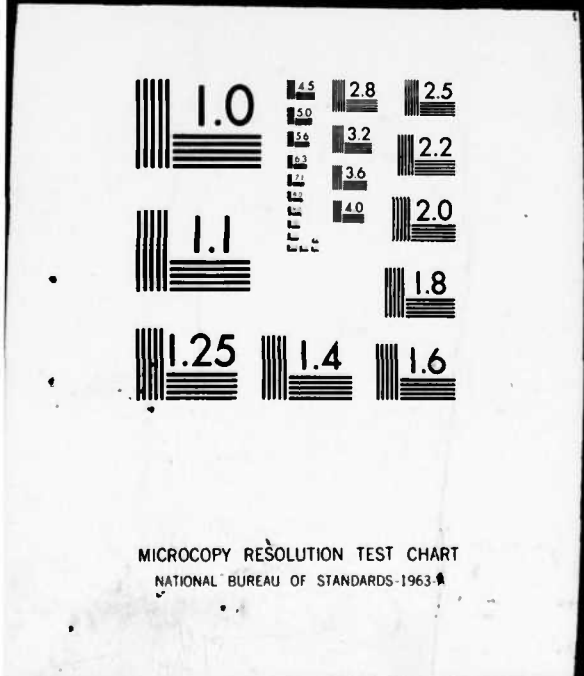
NL

| OF |
AD
A051853



END
DATE
FILED
4-78
DDC

5 | 85



ADA 051853

NTIS REPRODUCTION
BY PERMISSION OF
INFORMATION CANADA

CRDV RAPPORT 4091/78
DOSSIER: 3633H-003
FÉVRIER 1978

UNCLASSIFIED

1
3

R
DREV REPORT 4091/78
FILE: 3633H-003
FEBRUARY 1978

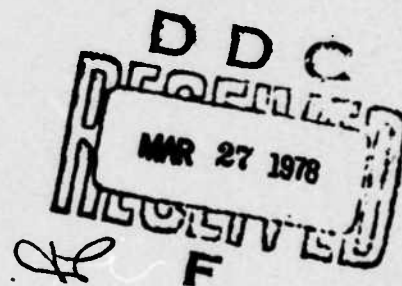
FREQUENCY AND AMPLITUDE CHARACTERISTICS OF
A HIGH-REPETITION-RATE HYBRID TEA-CO₂ LASER

J.-L. Lachambre

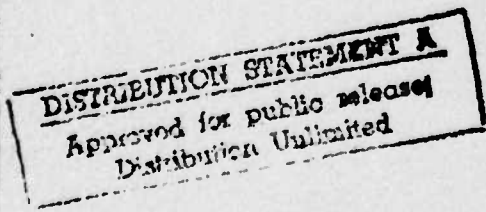
P. Lavigne

M. Verreault

G. Otis



AD NO. _____
DDC FILE COPY



BUREAU - RECHERCHE ET DEVELOPPEMENT
MINISTÈRE DE LA DÉFENSE NATIONALE
CANADA

NON CLASSIFIÉ

Centre de Recherches pour la Défense
Defence Research Establishment
Valcartier, Québec

RESEARCH AND DEVELOPMENT BRANCH
DEPARTMENT OF NATIONAL DEFENCE
CANADA

CRDV R-4091/78
DOSSIER: 3633H-003

UNCLASSIFIED

14

DREV-R-4091/78
FILE: 3633H-003

6

FREQUENCY AND AMPLITUDE

CHARACTERISTICS OF A HIGH-REPETITION-RATE

HYBRID TEA-CO₂ LASER

10

J.-L./Lachambre, P./ Lavigne, M./Verreault ✓ G./Otis

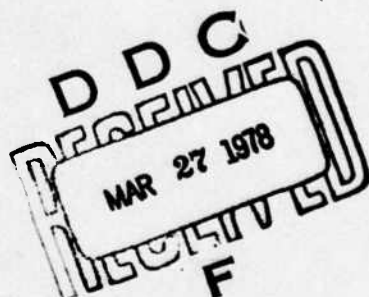
*Gen-Tec Inc., Québec

11

Feb 78

12

25 p.



CENTRE DE RECHERCHES POUR LA DEFENSE

DEFENCE RESEARCH ESTABLISHMENT

VALCARTIER

Tel: (418) 844-4271

Québec, Canada

February/février 1978

NON CLASSIFIÉ

DISTRIBUTION STATEMENT A

Approved for public release;
Distribution Unlimited

UNCLASSIFIED

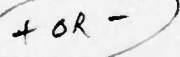
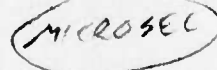
i

RESUME

Ce rapport présente les caractéristiques de l'impulsion de sortie d'un laser hybride CO₂ TEA à haute cadence de tir, tant du point de vue de la forme de son enveloppe que de la fréquence de sa porteuse. La stabilité de fréquence pendant l'impulsion même ainsi que d'une impulsion à l'autre y est expérimentalement déterminée pour des cadences allant jusqu'à 300 Hz. Il présente aussi l'analyse théorique et expérimentale du rétablissement du signal laser à ondes entretenues après la production de l'impulsion laser TEA. A 300 Hz, on observe une reproductibilité de fréquence à court terme de ± 2 MHz avec un taux de dérive d'environ 1.5 MHz/μs. Il étudie, en outre, les améliorations et les limites concernant la puissance et la cadence. (NC)

ABSTRACT

The envelope and frequency characteristics of the output pulse of a high-repetition-rate hybrid TEA-CO₂ laser are presented. Both the intrapulse and interpulse laser frequency stability are experimentally determined at repetition rates up to 300 Hz. The recovery of the CW laser signal following the generation of the TEA laser pulse is analyzed theoretically and experimentally. Short term reproducibilities of ± 2 MHz are observed at a pulse repetition rate of 300 Hz with initial chirp rates of about 1.5 MHz/μs. Improvements and limits on power and repetition rate are discussed. (U)

ACCESSION for				
NTIS	Classification			
DDC	B.R. Series			
UNANNOUNCED	<input type="checkbox"/>			
JUSTIFC:	<input type="checkbox"/>			
BY				
DISTRICTION, DRAFTING, COPY, ETC.				
Dist.	JUL			
<table border="1"> <tr> <td>A</td> <td></td> <td></td> </tr> </table>		A		
A				

UNCLASSIFIED
ii

TABLE OF CONTENTS

RESUME/ABSTRACT	i
1.0 INTRODUCTION	1
2.0 THE HYBRID LASER	1
3.0 EXPERIMENTAL APPARATUS	3
4.0 ENVELOPE CHARACTERISTICS	3
5.0 FREQUENCY CHARACTERISTICS	5
5.1 CW frequency stability	5
5.2 Interpulse frequency reproducibility	6
5.3 Intrapulse frequency stability	7
6.0 CW SIGNAL BEHAVIOR	11
6.1 Experimental observation of the CW signal recovery	11
6.2 Recovery simulation	12
7.0 CONCLUSION	16
8.0 ACKNOWLEDGEMENTS	16
9.0 REFERENCES	17
FIGURES 1 to 10	

UNCLASSIFIED
iii

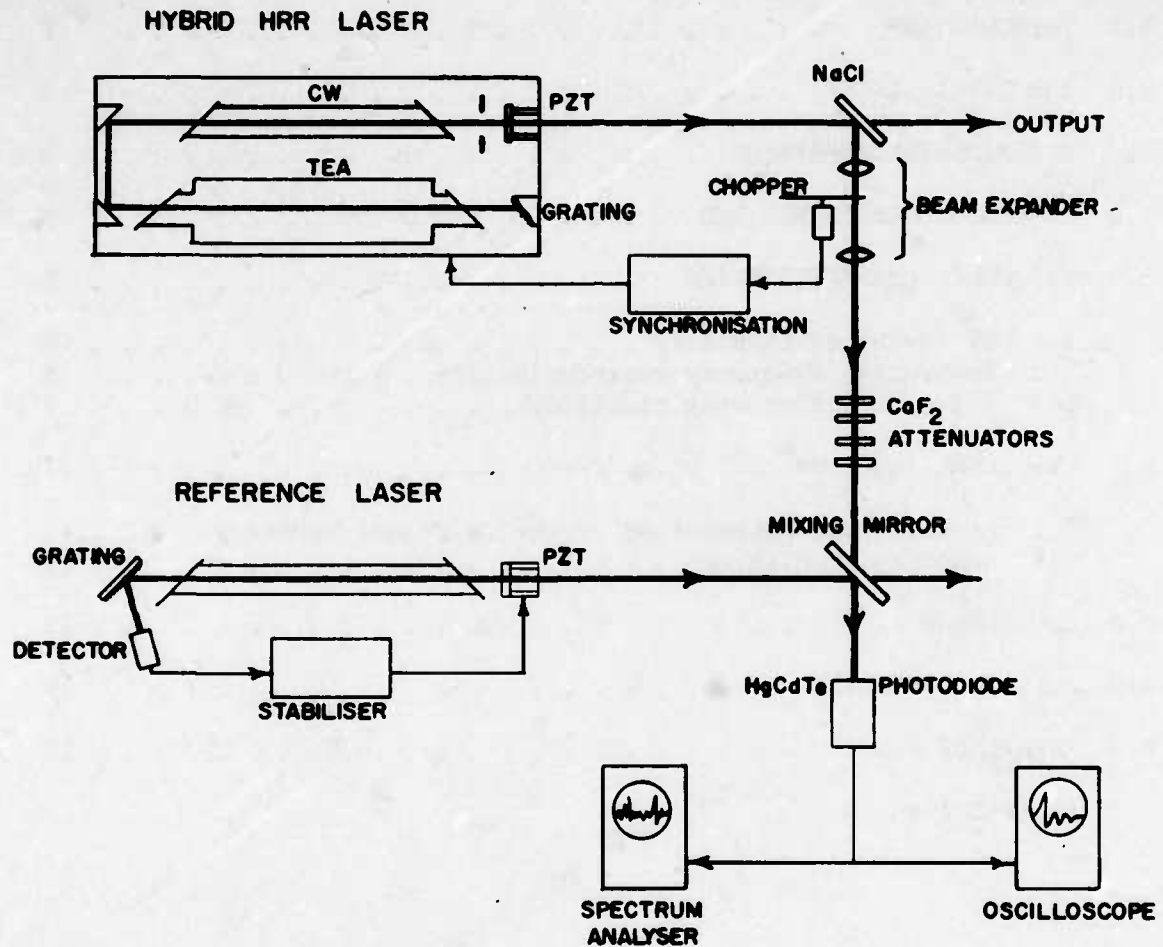


FIGURE 1 - Schematic of the apparatus

UNCLASSIFIED

1

1.0 INTRODUCTION

The emerging importance of TEA-CO₂ lasers in coherent detection systems, such as radars and velocimeters, has led us to study the various frequency selection and stabilization schemes that could force these powerful sources to emit on a single and stable frequency. Owing to their wide gain bandwidth, TEA-CO₂ lasers normally oscillate on several longitudinal modes of their resonator. Many mode-selection approaches have already been proposed; they utilize either multimirror cavity arrangements [1,2], injection techniques [3-5], or intracavity selective absorption [6] or amplification [7,8,9]. Among these schemes, the hybrid approach, that uses a TEA section and a low pressure gain tube in the same optical cavity, is especially attractive for stabilization purposes because it provides a continuous reference laser beam for long-term cavity stabilization [10].

It is the purpose of this paper to present the result of a thorough investigation of the power envelope and frequency performances of such a hybrid laser operated at pulse repetition frequencies suitable for preliminary application systems requiring high range or speed information rates. Both interpulse and intrapulse short-term frequency stability are measured to determine the ultimate long-term absolute stability achievable with appropriate servo compensation. The evolution of the CW laser signal between two consecutive TEA laser pulses is experimentally studied and the limitations imposed on the laser repetition rate by the gain recovery of the low-pressure section are discussed. The work was carried out between July and December 1976 under PCN 33H03 (formerly PCN 34A05) Sources for Coherent Ladars. The measurements presented in this document have been performed in the Gen Tec's laboratories on a hybrid TEA-CO₂ laser developed for DREV under contract 12SR-1430553.

2.0 THE HYBRID LASER

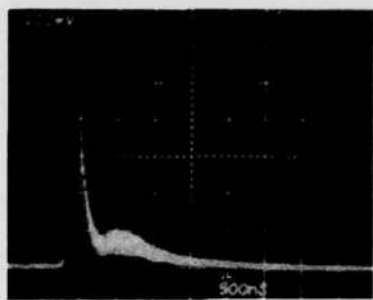
The hybrid laser system under study is schematically represented in Fig. 1. It consists essentially of a high-repetition-rate TEA-CO₂ discharge module mounted with a CW gain section in the same optical cavity. The TEA-CO₂ amplifier is a pin-grid double-discharge module that can be operated at repetition rates up to 350 Hz (Gen-Tec Model DD-300). A 35 m/s transverse gas flow of high uniformity circulates across the discharge area to ensure arc-free operation at high repetition rates. The TEA discharge system also comprises a gas regenerator which permits continuous operation at full average output power with a gas consumption lower than 1 l/min at 300 Hz. The active volume is approximately $1.4 \times 2.2 \times 43 \text{ cm}^3$, and the excitation energy is maintained constant at 77J/l. Small-signal gain coefficients of about 0.02 cm^{-1} are achieved in a He-N₂-CO₂ laser mixture of 8-1-1 at atmospheric pressure.

Selection of single longitudinal mode (SLM) is realized through the use of a low-pressure flowing-gas CW-CO₂ amplifier inserted in the cavity. This amplifier is a 1.2-cm ID water-cooled pyrex tube with an active length of 45 cm. At 9 torr, an optimum current of 20.5 mA produces a gain coefficient of 0.01 cm^{-1} in a He-N₂-CO₂ mixture of 8-1-1.

UNCLASSIFIED

2

a)



b)



c)

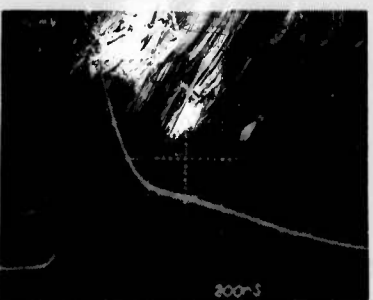


FIGURE 2 - Output power waveform with the low-pressure section off (a) and on (b,c)

UNCLASSIFIED

3

The optical resonator geometry is shown in Fig. 1. It consists of a 2.5-m folded path optical cavity thermally stabilized through the use of a combination of INVAR rods and compensation rings. The optical path is defined by a 100-grooves/mm concave grating (10-m radius), by two 45° fully reflecting plane mirrors and by a partially transmitting plane mirror (80% reflectivity) mounted on a piezoelectric translator for precise adjustment of the cavity length. The TEA-CO₂ and the low-pressure amplifiers are both sealed with ZnSe Brewster windows. The resonator structure is held on expansion-decoupling supports isolated against mechanical environmental vibrations through shock-absorbing pads. The laser oscillates in the fundamental TEM₀₀ mode at any repetition rate between 1 and 350 Hz with a pulse energy limited to 100 mJ due to the aperturing effect of the low-pressure tube.

3.0 EXPERIMENTAL APPARATUS

Figure 1 illustrates schematically the experimental arrangement used to study the envelope and frequency characteristics of the hybrid HRR laser. A 4%-portion of the hybrid laser output is 3X-expanded and attenuated through a stack of CaF₂ windows before being directed onto a high-speed (150 MHz) HgCdTe photodiode. In the mixing experiments, the output of a single-frequency line-tunable CW-CO₂ oscillator is added to the HRR-laser beam on a partial reflector and directed colinearly onto the same detector. The frequency of the local oscillator is stabilized at the CO₂ P(20) line-center by standard dithering techniques while the hybrid-laser cavity can be tuned over its 60-MHz intermode spacing by varying the bias voltage on the piezoelectric transducer. The output of the photodiode is amplified through a wide band amplifier and displayed either on a Tektronix 7904 oscilloscope or a Tektronix 7L12 spectrum analyzer.

Whenever necessary, the hybrid laser beam is mechanically blocked by a chopper wheel located at the focus of the first converging lens of the beam expander to obtain sharp transit times. The chopper rotating speed is arbitrarily adjusted so that its three blades obturate the beam at an effective rate of 270 Hz. A 2-mm blade-width is chosen to give an obturation time of about 50 μ s. Proper location of the chopper assembly leads to shutting and opening times of 2 μ s. Synchronizing electronics allow the firing of the TEA amplifier at any time of the obturation cycle and digital dividers provide means for varying the repetition rate as required.

4.0 ENVELOPE CHARACTERISTICS

With the intracavity low-pressure gain section turned off, the laser output consists of a 200-ns intense spike followed by a 1- μ s tail of much smaller amplitude. As shown in Fig. 2-a, this gain-switch pulse envelope, characteristic of TEA-CO₂ lasers, is modulated in amplitude by a high-frequency fine structure of periodicity 2L/c [16.7 ns].

UNCLASSIFIED

4

Careful observation of the mode-beating signal on expanded time scales suggests that 4 to 5 longitudinal modes are simultaneously oscillating in the cavity. By turning on and operating the low-pressure gain tube above threshold, the pulse shape is smoothed out, the leading spike is advanced by 500 ns and the peak power is reduced by almost a factor of two without significant changes in the pulse energy. Typical SLM power waveforms are shown in Figs. 2-b and 2-c. A close examination of the pulse envelope indicates that for correct adjustments of the resonator, the 60-MHz amplitude modulation, if there is any, is below the noise level of the detection system. This experimental limit, that amounts to 1% of the peak envelope, represents a longitudinal mode rejection in excess of 10^5 .

Detuning the cavity off the CO₂ line-center frequency has very little influence on the pulse envelope for most of the intermode frequency range. However, at detuning frequencies close to 30 MHz ($c/4L$), the power waveform exhibits a strong amplitude modulation at 60 MHz without any detectable harmonics. This observation suggests that only the two adjacent modes located almost symmetrically on either side of the low-pressure gain curve are simultaneously excited. For an initial CW power of one watt, this two-mode operation is restricted to a detuning zone about 5-MHz wide.

The above results indicate that the cavity must be stabilized around the CO₂-transition center-frequency for reliable SLM operation. Although much higher stability is required for radar or velocimetry applications, a stabilization of ± 25 MHz is sufficient to get high longitudinal-mode rejection.

The pulse repetition rate and the CW power level of the hybrid laser do not affect appreciably the pulse-shape characteristics. For operating pressures in the 5 to 10-torr range and CW powers ranging from 70 mW to 1 W, the output power waveform deformations do not exceed $\pm 5\%$ at any repetition rate from 1 to 300 Hz. For small gain in the low-pressure section, however, the tuning range for SLM operation is, as expected, narrower. As the CW laser gain is lowered across the threshold, the pulse envelope changes rapidly from a smooth curve to a spiky multimodal pattern with progressive time delay and peak power increases. Except when the low-pressure section is operated below threshold, the SLM envelope exhibits remarkable stability and reproducibility with time jitters smaller than ± 20 ns even at repetition rates up to 300 Hz. Such a performance is illustrated in Fig. 3 by an oscillogram showing 300 pulses superimposed over a one-second exposure.



FIGURE 3 - Multiple exposure oscilloscope showing 300 superimposed SLM pulses. The observation time is one second.

5.0 FREQUENCY CHARACTERISTICS

5.1 CW frequency stability

The frequency stability of the local oscillator is evaluated by beating its signal with the output of an identical reference source. Analysis of the heterodyne signal with the spectrum analyzer shows that each reference laser experiences frequency fluctuations of ± 0.6 MHz over a 1-s period; 30% of these variations are produced by the PZT modulation required for long term stabilization.

Heterodyning the reference laser with the output of the hybrid system shows frequency excursion up to ± 1.5 Mz over a 1-s period, when the TEA discharge and its gas handling system are turned off. Much larger frequency variations, attributed to thermal effects, are seen when the observation time is increased to a few minutes. As these drifts can be corrected using standard stabilization techniques, we limit our study to periods shorter than or equal to 1 second.

Operating the fans and circulating the gas in the TEA-discharge volume barely increase the short-term fluctuations. However, extreme care must be taken to avoid transmission of vibrations to the cavity structure from external elements. For example, the frequency excursion doubles when the fans used to cool the discharge circuit are improperly oriented. The beat frequency deviation between the reference laser and the CW section of the hybrid laser can be reduced, in the presence of gas circulation, to ± 2 MHz over a 1-s observation time by appropriate positioning of all the external perturbing elements.

UNCLASSIFIED

6

5.2 Interpulse frequency reproducibility

The frequency reproducibility of the TEA SLM pulse is then evaluated from the heterodyne beat signal between the TEA laser pulse and the reference source. Figure 4-a presents such a typical beat signal. On this oscillogram, the local oscillator illumination level corresponds to 120 mV. The TEA laser beam is attenuated to a peak level of approximately 5 mV to get resultant beat oscillations nearly symmetrical about the DC reference axis. Further increase of the local oscillator signal is not attempted because of possible damage to the photodiode. For all the TEA laser pulse frequency measurements, the low-pressure section of the hybrid laser is operated above threshold, delivering 1 W of CW output power. The study of the pulse-to-pulse frequency stability is conducted by probing, in each pulse, the same 200-ns portion starting 1 μ s after the beginning of the laser emission. This is illustrated in Fig. 4-a by the more luminous portion of the heterodyne signal trace. This portion of the pulse is selected by giving the appropriate delay to the second sweep of the dual-time base and then displayed on an expanded scale. Triggering the delayed sweep on the same part of the IF oscillation cycle allows the determination of the total frequency variation over a given exposure time. Figure 4-b represents typical results obtained by superposing such expanded traces taken over 1 s at a laser repetition rate of 7 Hz.

Measurements are made for various repetition rates and exposure times. No significant change in the frequency reproducibility is noticed when the sampling time is increased from 0.2 to 1 s and when the repetition rate is swept from 1 to 300 Hz. For all these cases, the total frequency variation is about ± 2 MHz. Heterodyning the reference laser with the CW signal of the hybrid system gives frequency fluctuations of the same order for similar exposure times. This similarity shows that, up to a repetition rate of 300 Hz, the TEA discharge itself has less influence on the interpulse frequency reproducibility than mechanical changes of the cavity structure. The fact that the frequency fluctuations do not decrease when reducing the exposure time down to 0.2 s indicates that the instability sources have high-frequency components and might consequently be mechanical vibrations. The much larger fluctuations, which are seen at long observation times and which are due to gas heating, further increase with the repetition rate. However, as these variations have spectral characteristics similar to those of the thermal cavity drift, they can be corrected through analogous compensation techniques.

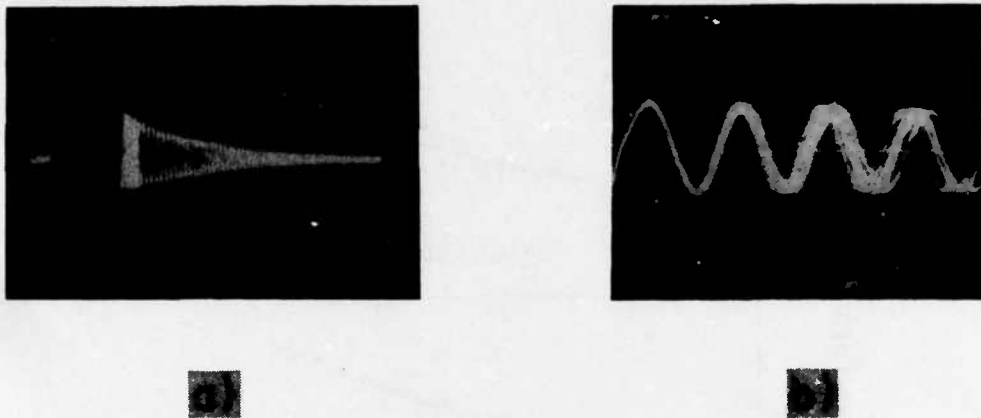


FIGURE 4 - a) Beating of the TEA laser pulse with the reference laser signal
b) One-second exposure of the expanded intensified portion of
oscillogram 4-a at 7 pulses/s

5.3 Intrapulse frequency stability

The intrapulse frequency stability of the hybrid system is investigated using the same heterodyne apparatus. During these experiments, the hybrid laser cavity is tuned at different frequencies on either the short or long-wavelength side of the CO₂ P(20) line, and the output of the detector is displayed on the oscilloscope. A typical heterodyne signal obtained with the cavity tuned on the low-frequency side of the local oscillator is shown in Fig 5. It is seen on this oscillogram that the resultant IF sweeps from approximately 10 MHz at the beginning of the pulse to about 4 MHz in the tail. This change represents an increase of the hybrid laser frequency of about 6 MHz.



FIGURE 5 - Time-resolved beat signal showing the intrapulse frequency chirp
at a pulse repetition rate of 300 Hz

UNCLASSIFIED

8

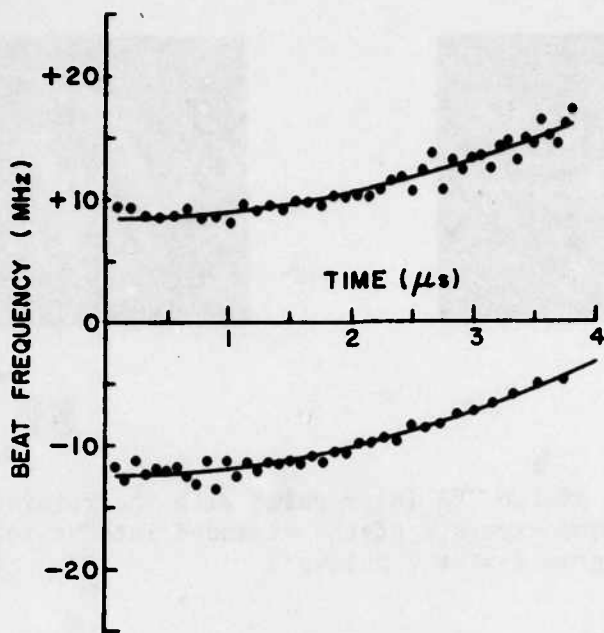


FIGURE 6 - Experimental instantaneous beating frequency for a positive and negative initial frequency offset (\circ). The solid lines represent fits of Eq. (1) with v_0 and b set respectively at 8.44 MHz and $0.52 \text{ MHz}/\mu\text{s}^2$ for the upper curve and -12.5 MHz and $0.575 \text{ MHz}/\mu\text{s}^2$ for the lower curve.

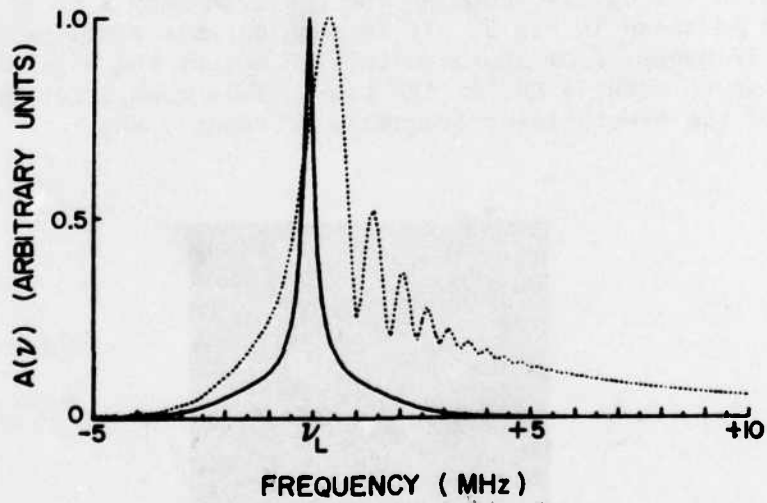


FIGURE 7 - Calculated amplitude Fourier spectrum of the TEA laser electric field with (----) and without (—) frequency chirping

UNCLASSIFIED

9

The approximate instantaneous frequency is determined from the period of each oscillation as measured at the zero crossing points and plotted as a function of the time elapsed since the beginning of the pulse. Figure 6 represents two typical examples of such a graph for which the starting frequency is on either side of the CO₂ line-center. It is seen that the hybrid laser frequency always increases. For small negative frequency offsets, the beat frequency decreases gradually, crosses the zero beat line and increases again. This behavior indicates that the resonant phenomena associated with the real part of the susceptibility of the gas have little influence on the frequency behavior of the system as any frequency chirp due to a resonant change of the index of refraction will change sign depending on the position of the initial cavity resonance with respect to the CO₂ line-center. Resonant effects as reported by Stiehl and Hoff [11] are not observed because of the low filling factors and the small frequency offsets.

Analysis of many sets of data indicates that curves of the form

$$\dot{\phi} = v_0 + bt^2, \quad (1)$$

fit very well the evolution of the instantaneous frequency $\dot{\phi}$. The variable v_0 is the beat frequency at the very beginning of the pulse while the constant b characterizes the chirp rate. The solid lines in Fig. 6 represent two typical fits obtained for positive and negative frequency offsets. The value of b does not change significantly with the repetition rate between 1 and 300 Hz, nor with the initial cavity resonant frequency v_0 between -20 and +20 MHz. The average value of b for all the experimental data is 0.575 MHz/ μ s² with a maximum deviation of ± 0.1 MHz/ μ s². This represents a total chirp of about 2.5 MHz during the first 2 μ s of the pulse which contain 90% of the pulse energy. This behavior must be compared to the change in refractive index appearing in the early stage of the discharge as measured by Dufour et al [12] in a similar electrode configuration using schlieren techniques.

The influence of the chirp on the hybrid laser frequency spectrum has been calculated from our experimental results. The broken and solid curves represented in Fig. 7 show the amplitude spectrum of the laser pulse with and without frequency chirping. In the former case, a frequency sweep of the form given by Eq. 1 is used. In this graph, v_L represents the laser carrier frequency at the beginning of the laser pulse. The frequency chirp increases the spectrum from 0.5 to about 2 MHz FWHM. In addition to this widening, there is a weak frequency displacement of the spectrum peak toward higher frequencies. The large wing of the spectrum on the high-frequency side represents the contribution of the pulse tail where the frequency chirp is more important.

UNCLASSIFIED

10

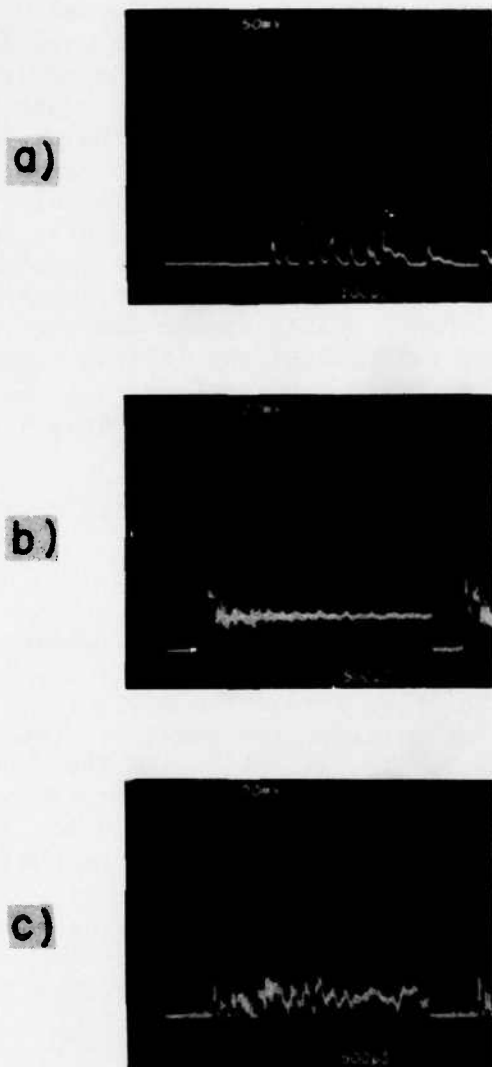


FIGURE 8 - a) and b) Typical recovery traces of the CW signal of the hybrid laser following the generation of the TEA laser pulse. c) Effect of a 15-MHz detuning with respect to the CO₂ line-center on the recovery signal.

UNCLASSIFIED

11

6.0 CW SIGNAL BEHAVIOR6.1 Experimental observation of the CW signal recovery

The behavior of the CW laser signal following the TEA laser pulse is observed directly on the HgCdTe photodiode while eliminating saturation of the detector by mechanically blocking the intense laser spike. In these measurements, the reference laser is turned off and the attenuators are reduced to allow linear detection of the CW signal, with a satisfactory signal-to-noise ratio. Firing the TEA laser section about the middle of the 50- μ s obturation time ensures that neither direct nor diffracted radiation of the pulse signal reaches the detector, as checked on the highest sensitivity scale. Typical power waveforms, recorded in this manner at a repetition rate of 270 Hz, are presented in Fig. 8 for a 9-torr pressure in the CW section. One retains from these oscilloscopes three major observations: first, a suppression of the laser oscillation during the first 300 μ s following the TEA laser pulse; second, at the end of this dead period, the appearance of a train of short and intense pulses for a few more hundred microseconds; and finally, a complete recovery of the CW signal 1 to 1.5 ms after the firing of the TEA discharge. Following the passage of the intense TEA laser pulse in the cavity, the CW gain section is left totally saturated, and laser emission is completely quenched. This dead time of the laser oscillation corresponds to the time required by the inversion to reach the threshold conditions under the continuous electronic pumping. With the mixture pressure set at 9 torr, the length of this quiet period increases from 300 μ s at 20.5 mA to 1 ms at 5 mA. This pumping current range corresponds roughly to gain coefficients varying from .01 to .002 cm⁻¹. At the end of this period, the onset of laser action takes the form of a decreasing pulse train superimposed to a progressive growth of the laser average power toward the steady state level. The initial multiple pulsing, similar in nature to that observed in ruby lasers [13], is attributed to successive gain switching induced by the continuously increasing gain in the low-pressure tube. The multiple-spike transient is damped over a period of about 1 ms toward the steady-state oscillation level. For active frequency stabilization, the total time required to reach the oscillation equilibrium imposes an upper limit of 700 Hz on the repetition rate of the laser system. This limit is further reduced to approximately 350 Hz, if one assumes a minimum of 1 ms for probing the laser frequency at equilibrium before triggering the next TEA laser pulse.

Detuning the cavity frequency leads to irregular pulsations and oscillations on the CW recovery signal, which retard the equilibrium point by many milliseconds. Figure 8-c shows the sort of distortion that is produced by a frequency detuning of \approx 15 MHz from the CO₂ line center at a pumping current of 20.5 mA. For lower tube current or correspondingly for smaller

UNCLASSIFIED

12

gain, the effect is even more accentuated. These irregular oscillations produced by the detuning of the laser cavity are not well understood; if they originate from dispersive effects in the CO₂ amplifying section, they are very likely accompanied by corresponding undesirable frequency deviations. However, these amplitude instabilities are not detrimental to active stabilization, since they just impose that the laser frequency be locked on the CO₂ transition center frequency.

6.2 Recovery simulation

In order to get a better understanding of the dynamics of the CW signal recovery, a simple theoretical model is used to simulate the main features of the laser field behavior following the TEA laser pulse formation. The model is used to determine the main factors that affect the CW signal recovery time and consequently to propose means for optimizing the repetition rate of hybrid CO₂ lasers.

The system of rate equations, that describes the evolution of the photon density and of the different populations in the cavity, is essentially based on the Stasz-De Mars equations [14] in which a constant is added to the population rates to simulate the continuous pumping of the inversion. Taking into account the relevant relaxation or exchange processes among the CO₂ and N₂ vibrational levels, the complete set of nonlinear differential equations becomes [15,16]:

$$\begin{aligned}\dot{I} &= -I/T_0 + \sigma c(N_b - fN_a)I + \sigma cN_b/V, \\ \dot{N}_a &= \sigma c(N_b - fN_a)I - \gamma_{ao}N_a + \gamma_{ba}N_b + W_a, \\ \dot{N}_b &= -\sigma c(N_b - fN_a)I - \gamma_{ba}N_b - \gamma_{bc}N_b + \gamma_{cb}N_c + W_b, \\ \dot{N}_c &= \gamma_{bc}N_b - \gamma_{cb}N_c + W_c,\end{aligned}$$

where I is the cavity photon density, N_a, the population density of the N₂ molecules in the v=1 vibrational mode, N_b, the population density of the CO₂ molecules in the v₃ mode and N_c, the total population density of the CO₂ molecules in the tightly coupled v₁ and v₂ modes. The fraction f of the group N_a that constitutes the lower laser level density amounts to approximately 1.5%. In these equations, V represents the cavity volume, T₀, the photon cavity lifetime and c, the speed of light. For the sake of simplicity, the laser transition is assumed to be homogeneously broadened with a radiative cross-section σ of the form [17,18]

$$\sigma = \frac{5 \times 10^{-17}}{x + .73y + .64z} \text{ cm}^2,$$

UNCLASSIFIED

13

where x, y, and z are respectively the CO₂, N₂ and He partial pressure in torr. In the above set of equations the constants γ_{ij} represent the various collisional deactivation or exchange rates from level i to level j and take the following values [15] at 300°K

$$\gamma_{ao} = (0.19x + 0.44y + 3.37z) \text{ ms}^{-1},$$

$$\gamma_{ba} = (0.35x + 0.106y + 0.085z) \text{ ms}^{-1},$$

$$\gamma_{bc} = 1.9y \text{ ms}^{-1} \text{ and } \gamma_{cb} = 1.7x \text{ ms}^{-1}.$$

Using finally the published electronic excitation rates for a typical E/N of 3×10^{-16} V-cm² [19], the pumping terms are then expressed by [20]:

$$W_a = (7.27 W_b) = xD_e \times 1.28 \times 10^9 \text{ s}^{-1} \text{ torr}^{-1},$$

$$\text{and } W_c = yD_e \times 8 \times 10^8 \text{ s}^{-1} \text{ torr}^{-1},$$

where D_e represents the plasma electronic density adjusted to fit the desired steady-state inversion. The complete set of differential equations is solved numerically by the coefficient integration method for stiff systems [21] and the resultant variables are normalized to their steady-state value. Since at the beginning the low-pressure medium is saturated by the TEA laser pulse, the initial conditions are set to:

$$I(0) = 0, N_c(0) = N_c(\infty)$$

$$\text{and } N_b(0) = fN_a(0) = \frac{f}{1+f} [N_a(\infty) + N_b(\infty)].$$

The results of a computer run that uses the experimental laser and cavity parameters are presented in Fig. 9. Here, the time origin coincides with the TEA laser pulse formation. The intensity waveform, calculated for a single-pass gain coefficient of 0.45 and a photon cavity lifetime of 53 ns in a 10-torr He-N₂-CO₂ mixture of 8-1-1, is to be compared with the experimental trace of Fig. 8-b. It is seen that the simulation reproduces quite well the main three experimental observations of the CW laser recovery: immediately after the TEA laser emission, the inversion builds up slowly and reaches the threshold in about 400 μs. Following that period of time over which the laser field is near the spontaneous emission level, a train of intense Q-switch pulses of decreasing amplitude are emitted under the continuous influence of the pumping. These oscillations are rapidly damped and both the inversion and the laser signal approach their steady state level in about 2.5 ms.

UNCLASSIFIED

14

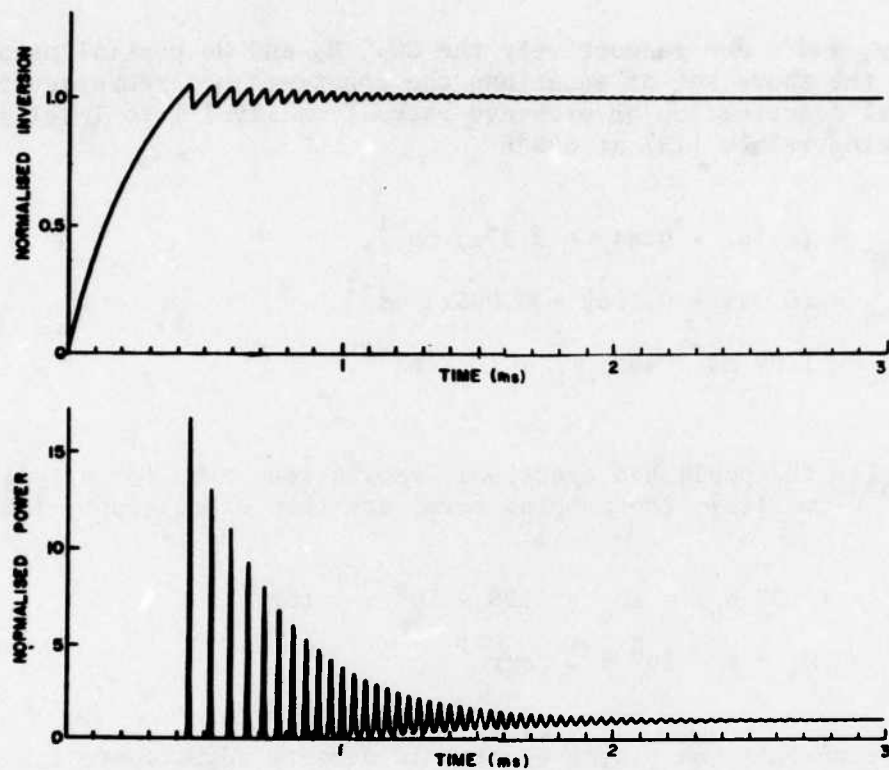


FIGURE 9 - Computer results giving the evolution of the recovery power signal and the inversion in the low-pressure section following the TEA laser pulse emission. ($T_0 = 53 \text{ ns}$, $\text{He-N}_2\text{-CO}_2 = 8-1-1 \text{ torr}$, $D_e = 4.6 \times 10^8 \text{ cm}^{-3}$).

The influence of the laser gain parameters on the signal recovery characteristic is studied by running the model program for different threshold and gain values. The results of such a computation are summarized in Fig. 10, where the dead time and the recovery time (0-90%) are plotted as functions of the single-pass gain coefficient for a fixed photon cavity lifetime of 53 ns. On this graph, both times are seen to diminish with a gain increase indicating that the repetition-rate capability of a hybrid CO₂ laser can be improved by augmenting the total CW gain in the cavity. Similar calculations with various threshold conditions show the same tendency. Finally, a simulation run at constant gain for various laser gas mixtures shows a strong dependence of the CW laser recovery time on the CO₂/N₂ ratio at identical gain. Since the N₂(v=1) molecules are not affected by the TEA laser pulse, they start transferring their energy to the CO₂ molecules immediately after gain saturation in such a way that

the higher the N₂ concentration the shorter the laser recovery time. Since the addition of a large quantity of N₂ normally decreases the CW gain for the same electronic pumping conditions, the optimization of the high-repetition-rate capabilities of a hybrid laser will result from a compromise between the N₂ concentration and the net cavity gain.

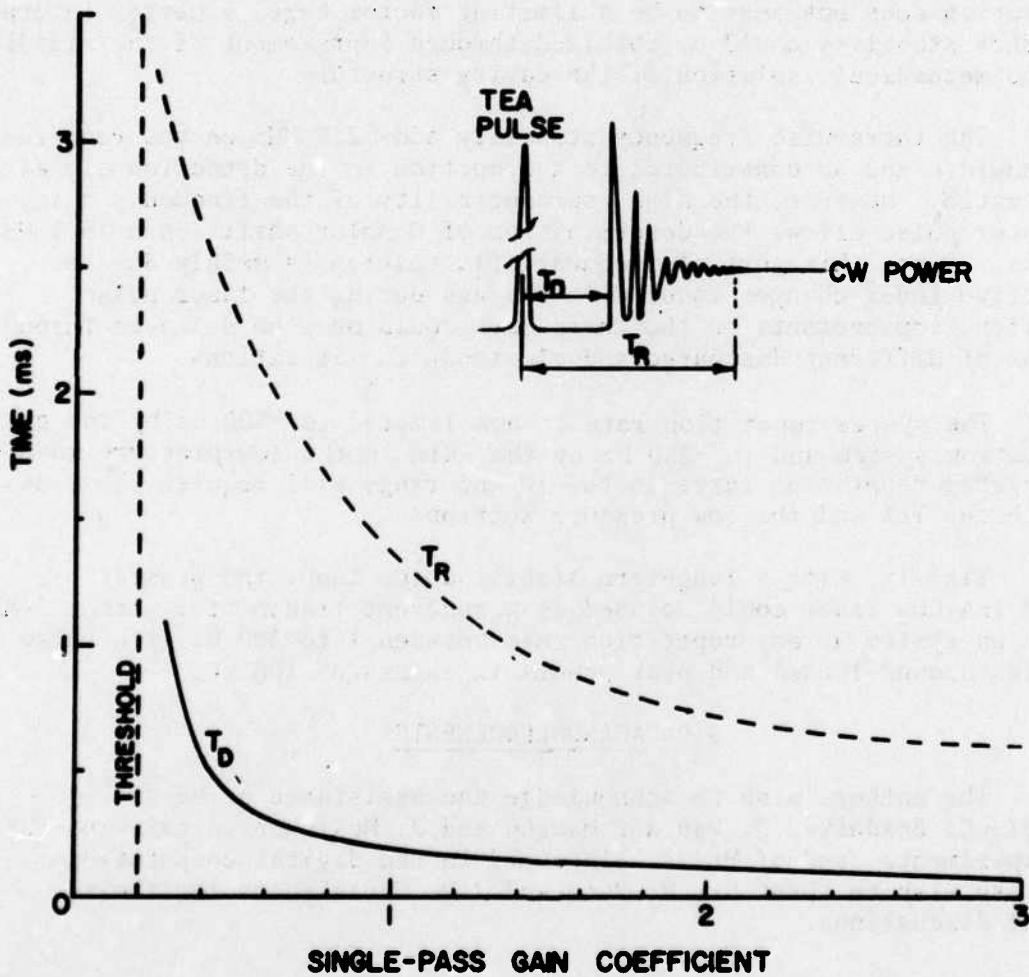


FIGURE 10- Calculated dead time T_D and recovery time T_R of the power recovery of the hybrid laser for various single-pass gain coefficients in an He-N₂-CO₂ mixture of 8-1-1 torr. ($T_0 = 53$ ns).

UNCLASSIFIED

16

7.0 CONCLUSION

Reliable SLM operation of a hybrid CO₂ laser has been demonstrated at repetition rates up to 350 Hz with output energies in the 100-mJ range. The use of larger bores in the low-pressure section together with large-mode resonator configurations should permit up to a threefold energy improvement with the same TEA laser head.

The short-term pulse-to-pulse frequency reproducibility of ± 2 MHz observed at any repetition rate from 1 to 300 Hz reflects the high stability of the laminar flow across the discharge. Since the gas circulation does not seem to be a limiting factor here, a better interpulse frequency stability could be obtained through improvement of the rigidity and the mechanical isolation of the cavity structure.

The intrapulse frequency stability adds 2.5 MHz on the required IF bandwidth and so contributes to a reduction in the detection signal-to-noise ratio. However, the high reproducibility of the frequency chirp during the laser pulse allows the determination of Doppler shifts down to 1 MHz or less. Since this sort of frequency fluctuation is mainly due to refractive-index changes induced in the gas during the laser pulse formation, improvements on the chirp rate could only be achieved through the use of different discharge and electrode configurations.

The system repetition rate is now limited to ~500 Hz by the gas circulation system and to ~350 Hz by the gain in the low-pressure module. Much higher repetition rates in the 10-kHz range will require the redesigning of both the TEA and the low-pressure sections.

Finally, with a long-term stabilisation loop, the present hybrid TEA-CO₂ laser could be used as a coherent transmitter with a 7-MHz IF detection system at any repetition rate between 1 to 300 Hz with pulse energies around 100 mJ and peak powers in excess of 100 kW.

8.0 ACKNOWLEDGEMENTS

The authors wish to acknowledge the assistance of Messrs. M. Noel, C. Bradette, R. Van der Haeghe and J. McKinnon in carrying out the experiments, and of Mr. A. Blanchard in the digital computations. They also wish to thank Dr. P. Pace and J.M. Cruickshank for their helpful discussions.

UNCLASSIFIED

17

9.0 REFERENCES

1. Smith, P.W., "Mode Selection in Lasers", Proc. IEEE, Vol. 60, No. 4, April 1972.
2. Weiss, J.A. and Goldberg, L.S., "Single Longitudinal Mode Operation of a Transversely Excited CO₂ Laser", IEEE Quantum Electron., Vol. QE-8, pp. 757-758, Sept. 1972.
3. Clobes, A.R., Berger, P.J., Brown, R.T. and Buczak, C.J., "Investigation to Determine Characteristics of a Stable-Frequency Pulse Regenerative-Amplifier CO₂ Laser Transmitter", United Aircraft Reserach Lab. Report No. AD-781737, Jan. 1974. UNCLASSIFIED
4. Meyer, J., "Single Mode CO₂-Laser Pulses of High Power", Phys. Lett. 58A, pp. 167-168, Aug. 1976.
5. Lachambre, J.-L., Lavigne, P., Otis, G. and Noël, M., "Injection Locking and Mode Selection in TEA-CO₂ Laser Oscillators", IEEE J. Quantum Electron., Vol. QE-12, pp. 756-764, Dec. 1976.
6. Nurmiikko, A., DeTemple, T.A. and Schwarz, S.E., "Single-Mode Operation and Mode Locking of High-Pressure CO₂ Lasers by Means of Saturable Absorbers", Appl. Phys. Lett., Vol. 18, pp. 130-132, Feb. 1971.
7. Gondhalekar, A., Holzhauer, E. and Heckenberg, N.R., "Single Longitudinal Mode Operation of High Pressure Pulsed CO₂ Lasers", Phys. Lett., Vol. 46A, pp. 229-230, Dec. 1973.
8. Girard, A., "The Effect of the Insertion of a CW, Low-Pressure CO₂ Laser into a TEA CO₂ Laser Cavity", Opt. Commun., Vol. 11, pp. 346-351, Aug. 1974.
9. Hamilton, D.C., James, D.J. and Ramaden, S.A., "A Repetitively Pulsed, Double Discharge TEA CO₂ Laser", J. Phys. E, Vol. 8, pp. 849-852, 1975.
10. Clobes, A.R., "Pulsed Laser Transmitter System", United Technologies Research Center Report No. R75-921840-12, Nov. 1975. UNCLASSIFIED
11. Stiehl, W.A. and Hoff, P.W., "Measurement of the Spectrum of a Helical TEA CO₂ Laser", Appl. Phys. Lett., Vol. 22, pp. 680-682, June 1973.
12. Dufour, M., Egger, H. and Seelig, W., "High Beam-Quality TEA Lasers", Opt. Commun. Vol. 19, pp. 334-338, Dec. 1976.
13. Statz, H., Luck, C., Shafer, C. and Ciftan, M., "Observations on Oscillations Spikes in Multimode Lasers", Advances in Quantum Electronics, Columbia Univ. Press, pp. 342-347, New York, 1961.

UNCLASSIFIED

18

14. Statz, H. and de Mars, G., "Transients and Oscillation Pulses in Masers", Quantum Electronics, Columbia Univ. Press, pp. 530-537, New York, 1960.
15. Moore, C.B., Wood, R.E., Bei-Lok Hu and Yardley, J.T., "Vibrational Energy Transfer in CO₂ Lasers", J. Chem. Phys., Vol. 46, pp. 4222-4231, June 1967.
16. Gilbert, J., Lachambre, J.-L., Rheault, F. and Fortin, R., "Dynamics of the CO₂ Atmospheric Pressure Laser with Transverse Pulse Excitation", Can. J. Phys., Vol. 50, pp. 2523-2535, 1972.
17. Arie, E., Lacombe, N. et Rossetti, C., "Spectroscopie par Source Laser. I. Etude expérimentale des Intensités et Largeurs des Raies de la Transition 00°1-(10°0, 02°0)_I de CO₂", Can. J. Phys. Vol. 50, pp. 1800-1804, 1972.
18. Abrams, R.L., "Broadening Coefficients for the P(20) CO₂ Laser Transition", Appl. Phys. Lett., Vol. 25, pp. 609-611, 1974.
19. Nighan, W.L. and Bennet, J.H., "Electron Energy Distribution Functions and Vibrational Excitation Rates in CO₂ Laser Mixtures", Appl. Phys. Lett., Vol. 14, pp. 240-243, April 1969.
20. Elliott, C.J., Judd, O.P., Lockett, A.M. and Rockwood, S.D., "Electron Transport Coefficients and Vibrational Excitation Rates for Electrically Excited CO₂ Gas Lasers", Los Alamos Report LA-5562-MS, April 1974. UNCLASSIFIED.
21. Liniger, W. and Willoughby, R.A., "Coefficient Integration Method for Stiff Systems of Ordinary Differential Equations", SIAM J. Numer. Anal., Vol. 7, pp. 47-66, March 1970.

CRDV R-4091/78 (UNCLASSIFIED)

Bureau - Recherche et Développement, Ministère de la Défense nationale, Canada.
CRDV, C.P. 880, Courcellette, Qué. G0A 1R0.

"Frequency and Amplitude Characteristics of a High-Repetition-Rate Hybrid
TEA-CO₂ Laser"

by J.-L. Lachambre, P. Lavigne, M. Verreault and G. Otis

Ce rapport présente les caractéristiques de l'impulsion de sortie d'un laser hybride CO₂ TEA à haute cadence de tir, tant du point de vue de son enveloppe que de la fréquence de sa portéeuse. La stabilité de fréquence pendant l'impulsion même n'empêche pas une impulsion à l'autre y est expérimentalement déterminée pour des cadences allant jusqu'à 300 Hz. Il présente aussi l'analyse théorique et expérimentale du rétablissement du signal laser à ondes entretenues après la production de l'impulsion laser TEA. A 300 Hz, on observe une reproductibilité de fréquence à court terme de ±2 MHz avec un taux de dérive d'environ 1.5 MHz/us. Il étudie, en outre, les améliorations et les limites concernant la puissance et la cadence. (NC)

CRDV R-4091/78 (UNCLASSIFIED)

Bureau - Recherche et Développement, Ministère de la Défense nationale, Canada.
CRDV, C.P. 880, Courcellette, Qué. G0A 1R0.

"Frequency and Amplitude Characteristics of a High-Repetition-Rate Hybrid

TEA-CO₂ laser"

by J.-L. Lachambre, P. Lavigne, M. Verreault and G. Otis

Ce rapport présente les caractéristiques de l'impulsion de sortie d'un laser hybride CO₂ TEA à haute cadence de tir, tant du point de vue de son enveloppe que de la fréquence de sa portéeuse. La stabilité de fréquence pendant l'impulsion même n'empêche pas une impulsion à l'autre y est expérimentalement déterminée pour des cadences allant jusqu'à 300 Hz. Il présente aussi l'analyse théorique et expérimentale du rétablissement du signal laser à ondes entretenues après la production de l'impulsion laser TEA. A 300 Hz, on observe une reproductibilité de fréquence à court terme de ±2 MHz avec un taux de dérive d'environ 1.5 MHz/us. Il étudie, en outre, les améliorations et les limites concernant la puissance et la cadence. (NC)

CRDV R-4091/78 (UNCLASSIFIED)

Bureau - Recherche et Développement, Ministère de la Défense nationale, Canada.
CRDV, C.P. 880, Courcellette, Qué. G0A 1R0.

"Frequency and Amplitude Characteristics of a High-Repetition-Rate Hybrid

TEA-CO₂ Laser"

by J.-L. Lachambre, P. Lavigne, M. Verreault and G. Otis

Ce rapport présente les caractéristiques de l'impulsion de sortie d'un laser hybride CO₂ TEA à haute cadence de tir, tant du point de vue de son enveloppe que de la fréquence de sa portéeuse. La stabilité de fréquence pendant l'impulsion même n'empêche pas une impulsion à l'autre y est expérimentalement déterminée pour des cadences allant jusqu'à 300 Hz. Il présente aussi l'analyse théorique et expérimentale du rétablissement du signal laser à ondes entretenues après la production de l'impulsion laser TEA. A 300 Hz, on observe une reproductibilité de fréquence à court terme de ±2 MHz avec un taux de dérive d'environ 1.5 MHz/us. Il étudie, en outre, les améliorations et les limites concernant la puissance et la cadence. (NC)

CRDV R-4091/78 (UNCLASSIFIED)

Bureau - Recherche et Développement, Ministère de la Défense nationale, Canada.
CRDV, C.P. 880, Courcellette, Qué. G0A 1R0.

"Frequency and Amplitude Characteristics of a High-Repetition-Rate Hybrid

TEA-CO₂ laser"

by J.-L. Lachambre, P. Lavigne, M. Verreault and G. Otis

Ce rapport présente les caractéristiques de l'impulsion de sortie d'un laser hybride CO₂ TEA à haute cadence de tir, tant du point de vue de son enveloppe que de la fréquence de sa portéeuse. La stabilité de fréquence pendant l'impulsion même n'empêche pas une impulsion à l'autre y est expérimentalement déterminée pour des cadences allant jusqu'à 300 Hz. Il présente aussi l'analyse théorique et expérimentale du rétablissement du signal laser à ondes entretenues après la production de l'impulsion laser TEA. A 300 Hz, on observe une reproductibilité de fréquence à court terme de ±2 MHz avec un taux de dérive d'environ 1.5 MHz/us. Il étudie, en outre, les améliorations et les limites concernant la puissance et la cadence. (NC)

DREV R-4091/78 (UNCLASSIFIED)

Research and Development Branch, Department of National Defence, Canada
DREV, P.O. Box 880, Courcellette, Que. (DA 1RD).

"Frequency and Amplitude Characteristics of a High-Repetition-Rate Hybrid
TEA-CO₂ Laser"
by J.-L. Lachambre, P. Lavigne, M. Verreault and G. Otis

The envelope and frequency characteristics of the output pulse of a high-repetition-rate hybrid TEA-CO₂ laser are presented. Both the intrapulse and interpulse laser frequency stability are experimentally determined at repetition rates up to 300 Hz. The recovery of the CW laser signal following the generation of the TEA laser pulse is analyzed theoretically and experimentally. Short term reproducibilities of ± 2 MHz are observed at a pulse repetition rate of 300 Hz with initial chirp rates of about 1.5 MHz/us. Improvements and limits on power and repetition rate are discussed. (U)

DREV R-4091/78 (UNCLASSIFIED)

Research and Development Branch, Department of National Defence, Canada
DREV, P.O. Box 880, Courcellette, Que. (DA 1RD).

"Frequency and Amplitude Characteristics of a High-Repetition-Rate Hybrid
TEA-CO₂ Laser"
by J.-L. Lachambre, P. Lavigne, M. Verreault and G. Otis

The envelope and frequency characteristics of the output pulse of a high-repetition-rate hybrid TEA-CO₂ laser are presented. Both the intrapulse and interpulse laser frequency stability are experimentally determined at repetition rates up to 300 Hz. The recovery of the CW laser signal following the generation of the TEA laser pulse is analyzed theoretically and experimentally. Short term reproducibilities of ± 2 MHz are observed at a pulse repetition rate of 300 Hz with initial chirp rates of about 1.5 MHz/us. Improvements and limits on power and repetition rate are discussed. (U)

DREV R-4091/78 (UNCLASSIFIED)

Research and Development Branch, Department of National Defence, Canada
DREV, P.O. Box 880, Courcellette, Que. (DA 1RD).

"Frequency and Amplitude Characteristics of a High-Repetition-Rate Hybrid
TEA-CO₂ Laser"
by J.-L. Lachambre, P. Lavigne, M. Verreault and G. Otis

The envelope and frequency characteristics of the output pulse of a high-repetition-rate hybrid TEA-CO₂ laser are presented. Both the intrapulse and interpulse laser frequency stability are experimentally determined at repetition rates up to 300 Hz. The recovery of the CW laser signal following the generation of the TEA laser pulse is analyzed theoretically and experimentally. Short term reproducibilities of ± 2 MHz are observed at a pulse repetition rate of 300 Hz with initial chirp rates of about 1.5 MHz/us. Improvements and limits on power and repetition rate are discussed. (U)

DREV R-4091/78 (UNCLASSIFIED)

Research and Development Branch, Department of National Defence, Canada
DREV, P.O. Box 880, Courcellette, Que. (DA 1RD).

"Frequency and Amplitude Characteristics of a High-Repetition-Rate Hybrid
TEA-CO₂ Laser"
by J.-L. Lachambre, P. Lavigne, M. Verreault and G. Otis

The envelope and frequency characteristics of the output pulse of a high-repetition-rate hybrid TEA-CO₂ laser are presented. Both the intrapulse and interpulse laser frequency stability are experimentally determined at repetition rates up to 300 Hz. The recovery of the CW laser signal following the generation of the TEA laser pulse is analyzed theoretically and experimentally. Short term reproducibilities of ± 2 MHz are observed at a pulse repetition rate of 300 Hz with initial chirp rates of about 1.5 MHz/us. Improvements and limits on power and repetition rate are discussed. (U)

ATE
MED